

archives
of thermodynamics

Vol. 44(2023), No. 1, 3–21

DOI: 10.24425/ather.2023.145874

Impact of raw liquid natural gas composition on combustion properties and emission characteristic

PAWEŁ CZYŻEWSKI*
RAFAŁ ŚLEFARSKI
JOANNA JÓJKA

Poznan University of Technology, Institute of Thermal Energy,
Piotrowo 3a, 60-965, Poznan, Poland

Abstract The article presents the results of numerical and analytical investigations of the influence of raw liquid natural gas (LNG) composition on parameters characterizing the combustion process. The high content of higher hydrocarbons influences the thermodynamic combustion process described with parameters like the adiabatic flame temperature, laminar flame speed and ignition delay time. A numerical study of the impact of LNG fuels on emission characteristics using the Cantera code has been performed. Results have shown that the change of grid natural gas to some types of liquid natural gas can result in an incomplete combustion process and an increase of emission of toxic compounds such as carbon monoxide and unburned hydrocarbons. For all investigated fuels the laminar flame speed rises by about 10% compared to natural gas, while the adiabatic flame temperature is nearly the same. The ignition delay time is decreased with an increase of ethane share in the fuel. The analysis of chemical pathways has shown that hydrogen cyanide and hydrogen formation is present, particularly in the high temperature combustion regimes, which results in an increase of nitric oxide molar fraction in flue gases by even 10% compared to natural gas. To summarize, for some applications, liquid natural gases cannot be directly used as interchangeable fuels in an industry sector, even if they meet the legal requirements.

Keywords: Toxic compounds; Fuel flexibility; Liquid natural gas; NO emission

*Corresponding Author. Email: pawel.czyzewski@put.poznan.pl

Nomenclature

d	–	relative density of fuel
HFL	–	higher flammability limit, %
HHV	–	higher heating value, MJ/Nm ³
LHV	–	lower heating value
LFL	–	lower flammability limit, %
MN	–	methane number
T	–	temperature, K
p	–	pressure, Pa
X_i	–	mole fraction of fuel components
T_A	–	adiabatic flame temperature, K
S_L	–	laminar flame speed, m/s
T_I	–	ignition temperature, K
t	–	time, s
t_d	–	ignition delay time
V_a	–	volume of theoretical combustion air, Nm ³
V_f	–	volume of fuel, m ³
Wb	–	Wobbe index, MJ/Nm ³

Greek symbols

λ	–	air excess ratio
ρ	–	density, kg/m ³

Acronyms

AVL	–	Adelson–Velsky and Landis method
EU	–	European Union
HC	–	hydrocarbons
HCN	–	hydrogen cyanide
LNG	–	liquid natural gas
NCN	–	cyanonitrene
NG	–	natural gas

1 Introduction

The achievement of the energy transition objectives enforced by the EU climate legislation [1] is based on the assumption of the use of natural gas (NG) as a transfer fuel between fossil fuels and a system based on the use of zero-emission sources. NG is approved as a carrier that allows the compensation of energy shortages from unstable renewable energy sources [2,3]. In view of the inadequacies of the available energy storage methods [2], natural gas is a fuel that offers the possibility of being utilized in systems with the possibility of high power generation with a rapid start-up time [5,6]. Until recently, this development was accompanied by attractive natural gas prices

that were not competitive with coal [7,8] while incurring lower carbon dioxide emission costs [3] making the use of natural gas for electricity generation a favorable method to reduce carbon dioxide emissions [4]. The generation of a unit of electricity in the combustion of natural gas contributes to two times less emission of carbon dioxide compared to the combustion of coal. These factors have resulted in a very dynamic process of increasing the share of energy produced from natural gas in the energy mix of many countries. A diametrical change in the NG market occurred in 2021, when, after a period of low prices for imported natural gas, a drastic several-fold increase in its price was observed. It was caused by an imbalance in the market resulting from the post-pandemic economic recovery and then the geopolitical situation related to Russia's military invasion of Ukraine. This has triggered a trend of turning away from Russian NG and the need to revise the existing energy policy towards seeking alternative solutions. One of them involves drastically increasing the use of natural gas transported by ships in the form of liquid natural gas (LNG) from countries distant from Europe.

Nowadays, LNG constitutes a large part of NG consumption and represents 36% [5] of the world natural gas market (for many countries covering even total fuel consumption) and is forecasted to get the majority of the gas market in 2035 (this trend can be accelerated by abandoning Russian NG). This situation implies that obstacles related to LNG consumption will be playing an important role, especially in the nearest future [6,7]. The diversification of natural gas supplies by increasing the share of LNG and gas from multiple geological deposits of different world regions requires analysis of the impact of their physical and chemical parameters on the combustion process and its emission.

In general imported liquefied gas contains more higher hydrocarbons [8] and is characterized by a different level of impurities. It involves many subsequent issues regarding their further utilization in energetic devices and the resulting emissions of carbon dioxide and toxic substances to the atmosphere. A great importance should be attached to the connection between the properties of the flammable mixture and final maintenance/emission outcomes. Many parameters describing the properties of natural gas and its utilization are applied [7]. These determining the most important impact are: lower heating value, energy content, combustion characteristics, impurities content, the Wobbe index, methane number [9], European standards compatibility, sulfur compounds content, dioxygen (O_2) and carbon dioxide (CO_2) shares, water and hydrocarbons dew points, damage risk, safety, burner controls, billing and Joule–Thomson effect.

Due to the fluctuations of nominal electricity production from renewable energy sources such as wind power and photovoltaics as well as the inadequacies of existing energy storage methods [2, 3], the import of electricity would not be able to replenish energy shortages in the absence of windy and overcast days. Most available energy storage technologies [10] require considerable financial, material and spatial efforts. For the time being, the most favourable method to overcome these obstacles to ensure the stable supply of electricity while reducing carbon emissions is the utilization of natural gas.

Unlike coal-fired steam boilers [11] supplying steam turbines, natural gas powered turbines [12] and engines have the ability to be quickly deployed and in the case of gas-steam systems, generate amounts of electricity comparable even to those fired with coal [13].

The energy policy of most industrialized countries is impacted by undertaking efforts to develop the potential of natural gas imports and to increase the diversification of supply sources. These include the planning and construction of many LNG terminals (14 units) [14] and pipelines connecting them with existing natural gas infrastructure [15]. The former European LNG market was focused on terminal operators in France, Spain, Italy, Belgium and the Netherlands. Recently, the Baltic Sea basin countries like Poland, Sweden, Lithuania and Finland have joined the group of European importers with their own LNG terminals.

LNG composition is usually different from the composition of natural gas supplied in onshore natural gas transmission networks (Table 1). This

Table 1: Example of liquid natural gas compositions at several LNG production locations [16]

Source name	LNG composition (%vol)				
	CH ₄	C ₂ H ₆	C ₃ H ₈	C ₄ H ₁₀	N ₂
Alaska	99.72	0.05	0.01	0.00	0.22
Algeria (Arzew)	86.98	9.35	2.33	0.63	0.71
Baltimore Gas&Electric	93.32	4.65	0.84	0.18	1.01
San Diego Gas&Electric	92.00	6.15	0.95	0.20	0.70
Qatar	90.90	6.43	1.66	0.74	0.27
Australia NWS	86.26	8.23	3.29	0.96	1.26
Malaysia	91.69	4.64	2.60	0.93	0.14
Russia – Sakhalin	92.54	4.47	1.97	0.95	0.07
Nigeria	91.60	5.64	2.15	0.58	0.03
Norway	92.03	5.75	1.31	0.45	0.46
Gas E (NG)	94.67	1.20	0.40	0.40	3.33

situation implies that obstacles related to LNG consumption will play an important role, especially in the nearest future.

This article deals with a comprehensive analysis of LNG mixed natural gases utilization in EU public transmission systems.

2 Methods

The gaseous fuel introduced to the EU countries' transmission and distribution networks should meet the quality parameters described in different legal regulations of individual Member States on special conditions for the functioning of the gas system [17]. These documents concern the minimum value of the higher heating value (HHV) for gaseous fuels with the Wobbe index (Wb). For high-methane natural gas of group E, the Wobbe index (Wb) is ranging from 45 MJ/m³ to 56.9 MJ/m³. Further regulations (ISO 13686:2013(en) [18]) define other quality parameters for gaseous fuels such as:

- hydrogen sulfide content < 7 mg/m³,
- mercaptan sulfur content < 16 mg/m³ (ISO 6326-3:1989(en) [19]),
- total sulfur content < 40 mg/m³ (ISO 6326-1:2007)(en), ISO 6326-5:1989(en)),
- content of mercury vapor < 30 µg/m³ (ISO 6978-1:2003(en) [20], ISO 6978-2:2003(en) [21]),
- dew point temperature +3.7°C (since 1st of Apr. to 30th of Sept.) and -5°C (since 1st of Oct. to 31st of March) (ISO 6327:1981(en) [22]).

One of the basic parameters determining the possibility of the various gaseous fuels replacement is the Wobbe index, which refers to the amount of chemical energy contained in the fuel stream. The values of basic quality parameters of gaseous fuels are based on the molar composition of the fuel obtained as a result of chromatographic analysis and standardized corresponding with ISO procedure (ISO 6976:2016 [23]).

The Wobbe index is calculated as the ratio of heat of combustion related to the unit of the volume of gaseous fuel to the square root of its relative density:

$$Wb = \frac{HHV}{\sqrt{d}}. \quad (1)$$

The relative gas density d stands for the ratio of the natural gas density and air density under the same reference conditions. The following calculations represent in general open systems placed inside manufacturing facilities, operating at the ambient pressure of 101325 Pa and temperature of 298.15 K. For the standardized volumetric flow (ISO 13443:1996 [24]), the reference values are corresponding to the normal gas state ($p = 101325$ Pa and $T = 273.15$ K).

The second group of physicochemical parameters characterizing the interchangeability of gaseous fuels are the operating parameters associated with the combustion process such as: the unitary amount of air needed to completely combust the supplied fuel (V_a/V_f), the lower and upper flammability limit of the gas mixture (LFL, HFL) and the methane number (MN).

The quantity of air needed to completely burn the fuel unit is determined based on the stoichiometric equations of the fuel oxidation process. Assuming a molar fraction of oxygen in the air at the level of 0.21, this dependence takes the form:

$$\frac{V_a}{V_f} = \frac{1}{0.21} \left[2X_{\text{CH}_4} + 0.5(X_{\text{CO}} + X_{\text{H}_2}) + \left(m + \frac{n}{4} \right) C_m\text{H}_n - X_{\text{O}_2} \right], \quad (2)$$

where X_i is the molar ratio of individual fuel components.

Lower and upper flammability limits refer to the lower and upper limit of the gaseous or vaporized fuel concentration in the air at a fixed temperature and pressure respectively which can lead to flame propagation. The values of LFL and HFL for fuel mixtures can be calculated based on the formulas:

$$\text{LFL} = \frac{1}{\sum_{i=1}^n \frac{x_i}{\text{LFL}_i}}, \quad (3)$$

and

$$\text{HFL} = \frac{1}{\sum_{j=1}^n \frac{x_j}{\text{HFL}_j}}, \quad (4)$$

where LFL_i and HFL_i are the lower and upper limits of individual components of gaseous fuel, and n is the number of flammable components.

The next important parameter which can be used as an interchangeability factor of gaseous fuels is methane number. The methane number describes resistance to auto-ignition of fuel and thus engine knock resistance when operating with a given fuel. For gaseous fuels, the value of MN is in

the range from 0 (for hydrogen) up to 100 (for methane). Knock resistance is rising with the MN increase. The value of methane number can be calculated based on many numerical codes created mostly on data delivered by Leiker *et al.* [25] or using the methodology presented by Kubesh [26]. For the purpose of industrial applications, a simplified method based on the ISO standard (ISO/TR 22302:2014) can be used. Other commonly used methods are the linear correlation method, hydrogen/carbon (H/C) ratio method or AVL method.

The last group of parameters which describe gaseous fuels are the thermodynamics properties of the combustion process such as the adiabatic flame temperature (T_A) [28], laminar flame speed (S_L) [29] and self-ignition temperature (T_I) [30]. These parameters define the selection of appropriate combustion technology and influence on the stability of the combustion process. The adiabatic flame temperature is the maximum temperature that can be obtained after the complete combustion process without heat losses to the surroundings. The value of T_A for different fuel blends can be calculated using numerical codes which take into account detailed combustion kinetics such as Chemkin-PRO or Cantera [31]. T_A depends on the initial parameters of substrates like temperature and pressure. Reaction mechanisms are based on the experimental measurements and validated [32, 33], where T_A , S_L and T_I are considered especially important parameters as characteristic mixture properties. The second parameter which can be obtained using numerical modelling of the combustion process is the laminar flame speed S_L [32]. The S_L is the velocity at which the flame front is moving in relation to the fresh gases in one-dimensional geometry [29]. The value of S_L is influenced by the fuel composition, excess of air as well as temperature and pressure of substrates (S_L decreases with the growth of pressure and increases with the growth of temperature of reagents). For stoichiometric flames at normal substrates conditions, S_L values range from 5 (for carbon monoxide) to 280 cm/s (for hydrogen), being around 42 cm/s for pure methane [33].

A parameter characterizing gaseous fuels which can be delivered from numerical modelling is the ignition temperature. According to the definition presented by Le Chaterier, T_I is the minimum temperature for which the amount of heat delivered from the combustion process is higher than the amount of heat lost to the preheating zone of reactants. For initial substrates' temperatures higher than the ignition temperature, a specific time interval could be noticed with a temperature peak as well as with the pressure rising. Proceeding further, autoignition is the spontaneous homo-

geneous ignition of the fuel-air mixture. The time for a mixture to reach autoignition is referred to as the ignition delay time, which is strongly dependent on the reactivity of the mixture [36–38].

In this work, the thermodynamic properties of gaseous fuels (T_A , S_L and T_I) were calculated using a 1D FreeFlame combustion model from the Cantera software libraries [34]. The mechanism UC SanDiego was chosen as a representation of C1–C4 combustion chemistry, which includes NO_x formation pathways [35]. The FreeFlame model represents a freely propagating flat reaction front including the reacting mixture movement and its transport properties. Calculations were conducted using a procedure, which was developed and validated for an axisymmetric methane-air flame with an approximate combustion chamber length of 0.5 m [36]. Estimation of the combustion chamber length was introduced as a linear grid, which was automatically refined with a slope and curvature control of 0.06 and 0.12, respectively. The calculated flame front propagated initially with the laminar burning velocity using mixture-averaged transport properties. The highest value of the temperature achieved by the modelled gas was the adiabatic flame temperature. This initial solution for each tested point was recalculated using a multicomponent transport in order to improve predictions of emissions and S_L . For the adiabatic flame temperature and the laminar flame speed, inlet mixture gas state parameters were kept at the constant level for all investigated LNG gases ($T = 300$ K and $p = 101325$ Pa), while the air excess ratio was changed in the range from 0.8 up to 1.8. Nitric oxide (NO) and carbon monoxide (CO) emission calculations were conducted using FreeFlame model with a radiative heat loss and a burner-stabilized BurnerFlame model. The BurnerFlame model was introduced to compare the CO emission when a fuel change was performed without an adjustment of the air stream. The air/fuel ratio of NG was a reference value. The performed simulations of non-adiabatic flames were in a better correlation to the mentioned NG burner tests [36] than those of perfectly insulated adiabatic flames, because of intensified heat exchange between the reacting mixture and surroundings. All emission values were recalculated to the dry reference base.

The ignition temperature and the ignition delay time (t_d) were calculated using a 0D model designed for the present investigations [37]. Each T_I as well as t_d value was obtained from a reactor filled with a perfectly stirred combustible mixture and surrounded by a non-expanding adiabatic wall. Raising the substrates' initial temperature to the mixture ignition temperature resulted in the initiation of the spontaneous exothermal reactions,

which affected the pressure and temperature of the modelled closed vessel. The calculated T_I was the lowest substrates' initial temperature for which the heat release was greater than the preheat zone consumption, and the combustion process started. The ignition delay time for selected fuels could be determined in two ways. First, as a relation between the reactor pressure change and time dp/dt , and second, as a specified temperature change given in absolute values ΔT . In the divergent formulation, the dp/dt function is examined and the simulation time corresponding to the maximum value of the function corresponds to the ignition delay time. For selected LNG and NG compositions, the initial temperature range from 800 K to 900 K was tested for a stoichiometric mixture with a 1 K step and an overall simulation time of 10 s with a 10^{-6} s time step. The mixture ignition temperature was marked as an initial mixture temperature if the combustion process occurred at a time below the total simulation time. Further investigations with the ignition delay time were performed for the before mentioned conditions. The initial temperature of the mixture was raised from 800 K to 1400 K with a 1 K step. The simulation time, where a significant temperature rise was observed as a mixture ignition delay time was compared to the value obtained by a divergent formulation approach. The temperature change between the following time steps ΔT at the end of mixture preheating was estimated at 5 K. The marked calculation point corresponds to the peak of the pressure function dp/dt and results in the gas temperature value of approximately 50% of the adiabatic flame temperature.

3 Results and discussion

3.1 Physicochemical properties of LNG

As it was mentioned in the previous chapter, the composition of natural gas obtained after the regasification process of LNG varies from that of natural gas delivered by the transition system. The major difference is the amount of high hydrocarbons that influence many physicochemical and thermodynamic parameters of fuel. The natural gas parameters received after the regasification process of LNG calculated based on Eqs. (1)–(4) are presented in Table 2. The methane number was found from the numerical code MWN_MN delivered by the European Association of Internal Combustion Engine Manufacturers [38].

As it is shown in Table 2, all investigated fuels fulfil the requirements of most EU market legislation acts with respect to the high heating value and

Table 2: Physico-chemical properties of LNG gases

LNG source name	ρ	d	HHV	Wb	V_a	LFL	HFL	MN
	(kg/m ³)	(–)	(MJ/Nm ³)	(MJ/Nm ³)	(Nm ³ _{air})	(%)	(%)	(–)
Alaska	0.717	0.555	39.66	53.24	9.5	5.3	15.0	99.8
Algeria (Arzew)	0.819	0.634	44.19	55.50	10.6	4.8	14.5	71.0
Baltimore Gas & Electric	0.764	0.591	41.38	53.81	9.9	5.1	14.9	82.8
San Diego Gas & Electric	0.771	0.597	41.72	54.01	10.0	5.0	14.9	81.4
Qatar	0.792	0.613	43.19	55.16	10.4	4.9	14.6	74.5
Australia NWS	0.833	0.645	44.50	55.41	10.7	4.7	14.5	68.6
Malaysia	0.796	0.616	43.43	55.35	10.4	4.9	14.6	73.0
Russia – Sakhalin	0.787	0.609	43.05	55.18	10.3	4.9	14.6	74.6
Nigeria	0.792	0.613	43.33	55.36	10.4	4.9	14.5	74.9
Norway	0.779	0.603	42.45	54.67	10.2	5.0	14.7	77.8
Gas E (NG)	0.754	0.583	39.36	51.54	9.4	5.4	15.4	90.4

Wobbe index. For all LNG fuels, the HHV was higher than 34 MJ/Nm³ and Wb was lower than 56.9 MJ/Nm³. According to Barczynski and Łaciak [39], the energetic devices for domestic solutions should be supplied with natural gas with the Wobbe index changing within the range of $\pm 5\%$, which gives the absolute margin value of 2.6 MJ/Nm³ for gas E (natural gas – base case). As it can be observed for LNG gases with a high content of high hydrocarbons, the difference between the value of Wb for certain fuels and gas E is even higher than 7% (LNG sources like: Qatar, Australia, Malesia and Algeria). It means that these fuels can be used as interchangeable fuels only for industrial devices where the easiest correction of the combustion process parameters is possible. Another important parameter is the amount of air delivered to the combustion process, which for the gas E group is equal to about 9.4–9.5 m³ of air per one Nm³ of fuel. The calculated value of V_a (air volume) has shown that for some LNG sources, this value is even more than 10% higher than that for natural gas delivered by transition networks, which introduces the risk of an incomplete oxidation process of fuel components and intensified emission of toxic compounds such as carbon monoxide (CO) or unburned hydrocarbons. The incomplete combustion process results also in a decrease of the combustion efficiency [40]. The higher content of hydrocarbons in the fuel causes a decrease of fuel knocking combustion resistance in a great part of energetic devices – reciprocating gas engines. For LNG fuels with the overall amount of high hydrocarbons above 7% (Qatar, Australia, Malesia and Algeria), the value of MN decreases

by even 30% compared to that of gas E. Complete interchangeability of the above-mentioned fuels requires modification of gas engine operating parameters such as the ignition delay time, engine boost and composition of combustion mixtures [41]. Even a slight shift of the range of engine working parameters can introduce recurring instabilities into the cycle, in some cases resulting in engine failure. In an extreme case, it can induce the engine stop. For example, the gas engine provider Westport Company require the usage of fuel with a minimum methane number of 75 for engines ISL G and ISX12 G [42].

In the case of lower and upper flammability limits for natural gas from the regasification process of LNG, the change is negligible. The higher amount of hydrocarbons in the fuels shifts the LFL to the lower values, which can result in an easier ignition of gas-fuel mixtures.

The influence of LNG composition on the laminar flame speed, the adiabatic flame temperature as well as ignition parameters has been numerically studied for five LNG gas compositions with Norway gas and grid natural gas as base cases (Table 3).

Table 3: Numerical calculation input

LNG source name	Fuel name	Initial calculation parameters		
		T_{sub}	p_{sub}	Air excess ratio
Algeria (Arzew)	LNG1	300 K	10^5 Pa	1–1.8
Qatar	LNG2			
Russia – Sakhalin	LNG3			
Baltimore Gas & Electric	LNG4			
Norway	LNG5			
Gas E	NG			

Results of numerical calculations of the laminar flame speed and adiabatic flame temperature are shown in Fig. 1 [16] (the air excess ratio was calculated according to formula $\lambda = (20.9\%)/(20.9\% - \text{O}_2 \text{ m}\%)$, where $\text{O}_2 \text{ m}\%$ is the measured volume value of oxygen in the dry exhaust gases). In both cases, it can be observed that for all investigated LNG gases the influence of fuel composition is negligible. For the calculation of T_A , the maximum difference was around 5 K (for LNG1) for the whole studied air excess ratio. It results from the adiabatic flame temperature definition, where the maximum temperature depends mostly on the amount of energy delivered from the fuel/air mixture and processes such as thermal dissociation and toxic

compounds' formation. For the investigated fuels, the amount of energy delivered from 1 kg of the fuel/air mixture was almost constant (ranging from 3.85 MJ/kg up to 4.04 MJ/kg).

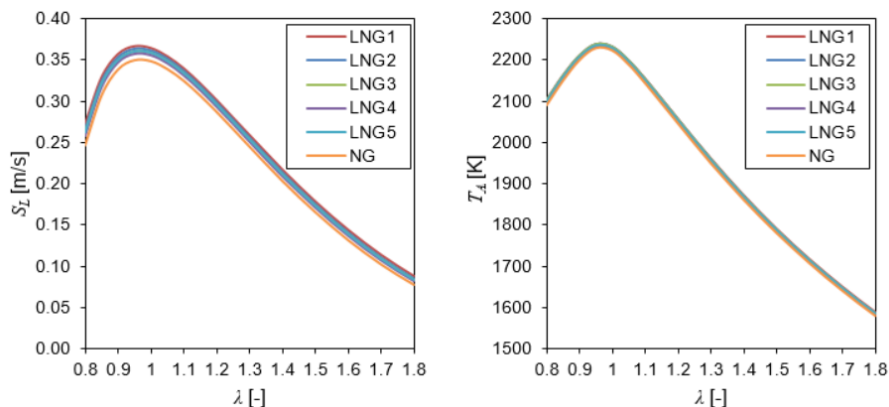


Figure 1: Laminar flame speed and adiabatic flame temperature *versus* air excess ratio.

In the case of laminar flame speed, the most significant change of S_L value was observed in rich and stoichiometric conditions. The increase of HC share in the LNG fuels induced an increase of the S_L value even by 10% for LNG1 (the highest content of ethane). It has been established that for combustible mixtures of a similar structure, the laminar flame speed is directly correlated with the adiabatic flame temperature. In the analyzed cases, where the calculated T_A and mass burning rate are very similar for all investigated LNG fuels, there is a secondary effect which causes a deviation in the laminar flame speed. Since liquid natural gas is a mixture of simple alkanes (C1–C4), the S_L deviation is caused mainly by the global consumption rate and density-compensated diffusivity [43].

The next analyzed parameters for the selected fuels (Table 3) are the ignition temperature and ignition delay time. For the estimation of T_I and t_d , the procedure described in Section 2 was used. The calculated value of ignition temperature was at the same level in the range from 801 K to 806 K for the 10 s ignition induction time. The influence of LNG composition on the value of ignition delay time (Fig. 2) was observed.

For the whole investigated range of air excess ratio, the shorter ignition delay time was observed for LNG1 while the ignition process of NG was delayed by about 0.05 s. It was also noticed that the most significant impact on the value of ignition time has the amount of ethane in the fuel. This is

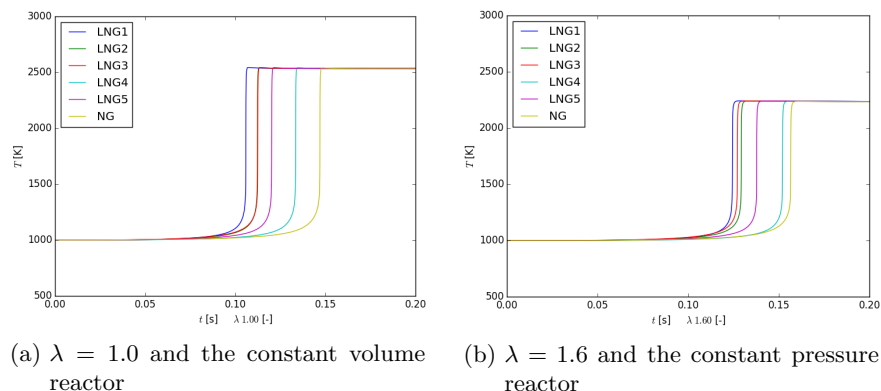


Figure 2: Ignition delay time for investigated fuels.

due to the character of the ethane oxidation process where a larger quantity of ethylene is produced and consequently more vinyl radicals are formed. They are more reactive than acryl radicals released from the combustion of longer chain alkenes (e.g., propane, butane). Moreover, slight differences in the maximum pressure value were observed for the combustion of provided mixtures in the constant volume.

To conclude, it can be said that for all studied LNG compositions, a significant influence on the combustion parameters such as T_A , S_L and T_i was not observed. It suggests that from this point of view, the LNG could be used interchangeably without loss of flame stability.

3.2 Emission characteristics

A second important parameter describing the combustion process is the emission of toxic compounds such as nitric oxides, carbon monoxide and unburned hydrocarbons. In this work, the emission analysis was divided into two parts. In the first, only the influence of fuel composition was taken into account. The results of nitric oxides and carbon monoxide emission are presented in Fig. 3.

Based on the results of numerical calculations of toxic compounds presented in this figure it can be noticed that the amount of air delivered to the combustion process has the most significant impact on the emission value. The impact of LNG composition (impact of the amount of high hydrocarbons) is most visible for rich and close to stoichiometric conditions. The nitric oxide emission rises by about 10% (25 ppm) for LNG1 and LNG5

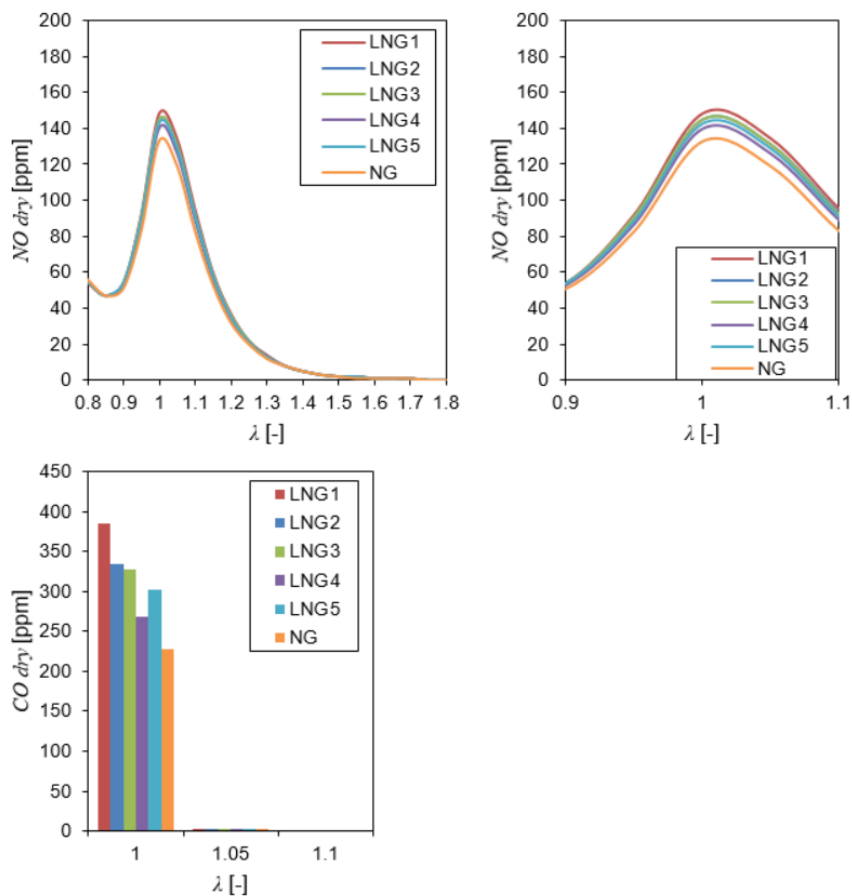


Figure 3: Emission characteristic of NO and CO; 1D FreeFlame with the radiative heat loss.

compared to NG. As it was presented before, T_A is almost constant for all analyzed fuels. Therefore, it can be concluded that an increase of nitric oxide (NO) emissions is determined by a pathway other than thermal, probably by a prompt mechanism. The study on the combustion process of alkanes [44] has shown an increased amount of hydrogen cyanide (HCN) in the flame in the case of combustion of ethane, propane and butane in rich conditions. HCN originating from NCN (cyanonitrene) reactions is then the precursor of NO formation [45] according to the aforementioned prompt mechanism. The influence of LNG composition on carbon monoxide is negligible in the whole range of considered air excess ratios.

In the second case, constant amounts of air equal to 12.3, 12.9 and 13.5 kg_{air}/Nm_{fuel}³ corresponding to air excess ratio equal to 1.05, 1.1 and 1.15 (for NG combustion process) were taken as initial parameters of the combustion process. Conditions of the atmospheric pressure and constant temperature of substrate $T = 300$ K were used. This scenario simulates the real operating conditions of an energetic device for which the fuel type has been changed without any regulation. As it can be seen in Fig. 4, the fuel change from natural gas to LNG fuels resulted in a sharp increase of carbon monoxide emissions, which indicates an incomplete combustion process.

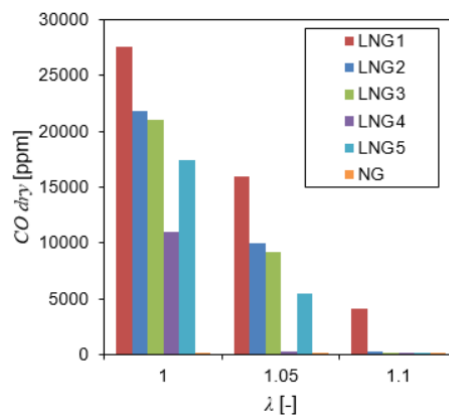


Figure 4: Carbon monoxide emission for a constant amount of air delivered to the combustion process; 1D BurnerFlame.

It can be noticed that even for the combustion process of NG taking place with the air excess ratio $\lambda = 1.1$ (2% of O₂ in dry flue gases), the introduction of LNG1 (instead NG) results in the emission of CO of about 4000 ppm. For the combustion processes with a lower air excess ratio, the molar fraction of carbon monoxide reached even a few per cent. Next to carbon monoxide, a significant amount of hydrogen (up to 1%) is observed. Such combustion processes cause a decrease of the combustion efficiency (up to 10%) [40] and can be dangerous for safety of the maintenance personnel.

4 Conclusions

The composition of LNG depends on the source location and varies mainly by different amounts of high hydrocarbons. As it was shown, the amount of high hydrocarbons in the fuel can reach even 10% of the molar fraction,

which has an influence main parameters of the combustion process and emission characteristics. The impact of LNG composition on parameters like the lower and upper flammability limits, adiabatic flame temperature, laminar flame speed or ignition temperature is negligible and does not influence the flame stability. The increased number of high hydrocarbons, especially the amount of ethane, can even improve the fuel ignition process and lead to a more stable combustion process. On the other side, an increase of hydrocarbons in LNG indicates a significant decrease of fuel resistance to knocking combustion processes, which disqualifies the utilization of raw LNG as a potential fuel for reciprocating gas engines. It was presented that replacing natural gas with LNG increased the nitric oxides emission even by a few percent.

The results showed that in the case of raw liquid natural gas introduced as a fuel to energy devices operating with a low air excess ratio, a significant increase in emission of carbon monoxide (even by a few per cent) and unburned hydrocarbons was noticed. It decreases the combustion efficiency and leads to the introduction of a large amount of toxic compounds into the environment.

Summarizing, it can be said that raw LNG can be used as interchangeable fuel to natural gas. However, in some industrial applications additional modifications are required, for example introduction of anti-knocking combustion systems, control of operating parameters or introduction of additional toxic compounds reduction systems.

Received 8 August 2022

References

- [1] Looi K.K., Baheta A.T., Habib K.: *Experimental performance and comfort analyses of photovoltaic thermoelectric system in a room air-conditioning application*. Heat Transf. Eng. **42**(2021), 1172–83. doi: [10.1080/01457632.2020.1777010](https://doi.org/10.1080/01457632.2020.1777010)
- [2] Mosiężny J., Ziegler B., Czyżewski P.: *Numerical study of heat and mass flow in phes layered bed heat storage*. Int. J. Numer Methods Heat Fluid Flow. **30**(2020), 6, 3199–3209.
- [3] Li H., Chen L., Wang D., Zhang H.: *Analysis of the price correlation between the international natural gas and coal*. Energy Procedia **142**(2017), 3141–6. doi: [10.1016/j.egypro.2017.12.376](https://doi.org/10.1016/j.egypro.2017.12.376)
- [4] Mac Kinnon M.A., Brouwer J., Samuelsen S.: *The role of natural gas and its infrastructure in mitigating greenhouse gas emissions, improving regional air quality, and renewable resource integration*. Prog. Energy Combust. Sci. **64**(2018), 62–92. doi: [10.1016/j.pecs.2017.10.002](https://doi.org/10.1016/j.pecs.2017.10.002)

- [5] *Natural gas trade via pipeline and LNG shipping worldwide from 2000 to 2019, with a forecast until 2050* <https://www.statista.com/statistics/1165885/global-natural-gas-trade-by-flow-type/> (accessed March 16, 2020).
- [6] Lisowski F., Lisowski E.: *Design of internal supports for double-walled liquefied natural gas road tanker*. *Heat Transf. Eng.* **43**(2021), 238–47. doi: [10.1080/01457632.2021.1874653](https://doi.org/10.1080/01457632.2021.1874653)
- [7] Akinsipe O., Anozie A., Babatunde D.: *A study of LNG processes to determine the effect of end flash systems on efficiency*. *Arch. Thermodyn.* **41**(2020), 2, 35–63. doi: [10.24425/ather.2020.132959](https://doi.org/10.24425/ather.2020.132959)
- [8] Xu S., Chen X., Fan Z., Chen Y., Nie D., Wu Q.: *The influence of chemical composition of LNG on the supercritical heat transfer in an intermediate fluid vaporizer*. *Cryogenics (Guildf)* **91**(2018), 47–57. doi: [10.1016/j.cryogenics.2018.01.011](https://doi.org/10.1016/j.cryogenics.2018.01.011)
- [9] Roy P.S., Ryu C., Park C.S.: *Predicting Wobbe index and methane number of a renewable natural gas by the measurement of simple physical properties*. *Fuel* **224**(2018), 121–7. doi: [10.1016/j.fuel.2018.03.074](https://doi.org/10.1016/j.fuel.2018.03.074)
- [10] Liu C., Li F., Ma L.P., Cheng H.M.: *Advanced Materials for Energy Storage*. *Adv. Mater.* **22**(2010), 28–62. doi: [10.1002/adma.200903328](https://doi.org/10.1002/adma.200903328)
- [11] Hernik B., Zablocki W.: *Numerical research of combustion with a minimum boiler load*. *Arch. Thermodyn.* **41**(2020), 4, 93–114. doi: [10.24425/ather.2020.135855](https://doi.org/10.24425/ather.2020.135855)
- [12] Joachimiak D., Frackowiak A.: *Experimental and numerical analysis of the gas flow in the axisymmetric radial clearance*. *Energies* **13**(2020), 21, 5794. doi: [10.3390/en13215794](https://doi.org/10.3390/en13215794)
- [13] Kindra V.O., Milukov I.A., Shevchenko I.V., Shabalova S.I., Kovalev D.S.: *Thermodynamic analysis of cycle arrangements of the coal-fired thermal power plants with carbon capture*. *Arch. Thermodyn.* **42**(2021), 4, 103, 21. doi: [10.24425/ather.2021.139653](https://doi.org/10.24425/ather.2021.139653)
- [14] Rogers D., Nelson R., Howell N.: *LNG in Europe: An Overview of European Import Terminals*. King & Spalding LLP, Georgia 2018.
- [15] Wood D.A.: *A review and outlook for the global LNG trade*. *J. Nat. Gas Sci. Eng.* **9**(2012), 16–27. doi: [10.1016/j.jngse.2012.05.002](https://doi.org/10.1016/j.jngse.2012.05.002)
- [16] Agentschap NL.: *Gas Composition Transition Agency Report 2013. The status of the transition to high-calorific-value gas*. Ministerie van Economische Zaken, 2013.
- [17] EN 16726:2015 (E): *Gas infrastructure – Quality of gas – Group H – European Standard – Final Draft*. 2015.
- [18] ISO 13686:2013(en) *Natural gas – Quality designation*. 2013.
- [19] ISO 6326-3:1989 *Natural gas – Determination of sulfur compounds – Part 3: Determination of hydrogen sulfide, mercaptan sulfur and carbonyl sulfide sulfur by potentiometry*. 1980.
- [20] ISO 6978-1:2003 *Natural gas – Determination of mercury – Part 1: Sampling of mercury by chemisorption on iodine*. 2003.
- [21] ISO 6978-2:2003 *Natural gas – Determination of mercury – Part 2: Sampling of mercury by amalgamation on gold/platinum alloy*. 2003.

- [22] ISO 6327:1981 *Gas analysis – Determination of the water dew point of natural gas – Cooled surface condensation hygrometers*. 1981.
- [23] ISO 6976:2016 *Natural gas – Calculation of calorific values, density, relative density and Wobbe indices from composition*. 2016.
- [24] ISO 13443:1996 *Natural gas – Standard reference conditions*. 1996.
- [25] Leiker M., Christoph K., Rankl M., Cartellieri W., Pfeifer U.: *The evaluation of the antiknocking property of gaseous fuels by means of the methane number and its practical application to gas engines*. In: Proc. 9th Int. Cong. on Combustion Engines, Stockholm 1971.
- [26] Kubesh J., King S., Liss W.: *Effect of gas composition on octane number of natural gas fuels*. SAE Tech. Pap. 922359, 1992. doi: [10.4271/922359](https://doi.org/10.4271/922359)
- [27] ISO 15403-1:2006 *Natural gas – Natural gas for use as a compressed fuel for vehicles – Part 1: Designation of the quality*. 2006.
- [28] Kayadelen H.K.: *A multi-featured model for estimation of thermodynamic properties, adiabatic flame temperature and equilibrium combustion products of fuels, fuel blends, surrogates and fuel additives*. Energy **143**(2018), 241–56. doi: [10.1016/j.energy.2017.10.106](https://doi.org/10.1016/j.energy.2017.10.106)
- [29] Wei W., Yu Z., Zhou T., Ye T.: *A numerical study of laminar flame speed of stratified syngas/air flames*. Int. J. Hydrogen Energy. **43**(2018), 9036–45. doi: [10.1016/j.ijhydene.2018.03.167](https://doi.org/10.1016/j.ijhydene.2018.03.167)
- [30] Fieweger K., Blumenthal R., Adomeit G.: *Shock-tube investigations on the self-ignition of hydrocarbon-air mixtures at high pressures*. Symp. Combust. **25**(1994), 1579–1585. doi: [10.1016/S0082-0784\(06\)80803-9](https://doi.org/10.1016/S0082-0784(06)80803-9)
- [31] Goodwin D., Moffat H., Speth R.: *Cantera: An Object-Oriented Software Toolkit For Chemical Kinetics, Thermodynamics, And Transport Processes. Version 2.3.0*. 2017. doi: [10.5281/zenodo.170284](https://doi.org/10.5281/zenodo.170284)
- [32] Sher E., Levinzon D.: *Scaling-down of miniature internal combustion engines: Limitations and challenges*. Heat. Transf. Eng. **26**(2005), 1–4. doi: [10.1080/01457630591004780](https://doi.org/10.1080/01457630591004780)
- [33] Hermanns R.T.E., Konnov A.A., Bastiaans R.J.M., De Goey L.P.H., Lucka K., Köhne H.: *Effects of temperature and composition on the laminar burning velocity of CH₄+H₂+O₂+N₂ flames*. Fuel **89**(2010), 114–21. doi: [10.1016/j.fuel.2009.08.010](https://doi.org/10.1016/j.fuel.2009.08.010)
- [34] Goodwin D.G., Moffat H.K., Schoegl I., Speth R.L., Weber B.W.: *Cantera: An object-oriented software toolkit for chemical kinetics, thermodynamics, and transport processes. Version 2.6.0*. 2022. doi: [10.5281/zenodo.6387882](https://doi.org/10.5281/zenodo.6387882)
- [35] *Chemical-Kinetic Mechanisms for Combustion Applications*. Univ. Calif., San Diego 2022.
- [36] Ślęfarski R.: *Study on the combustion process of premixed methane flames with CO₂ dilution at elevated pressures*. Energies **12**(2019), 3. doi: [10.3390/en12030348](https://doi.org/10.3390/en12030348)
- [37] Smith G.P., Golden D.M., Frenklach M., Moriarty N.W., Eiteneer B., Goldenberg M., Bowman C.T., Hanson R.K., Song S., Gardiner W.C., Lissianski J.V.V., Zhivey Q.: *GRI-Mech 3.0*. 2020 <http://combustion.berkeley.edu/gri-mech/> (accessed March 10, 2021).

- [38] <https://www.euromot.eu/publication-and-events/publications/> (accessed Jan. 16, 2019).
- [39] Barczyński A., Łaciak M.: *Interchangeability of gaseous fuels (natural gas)*. Wiadomości Naft. Gazow. **8**(2014), 196 (in Polish).
- [40] Odgers J., Kretschmer D.: *Gas turbine fuels and their influence on combustion*. Abacus Press, Swinburne 1986.
- [41] Mozgovoy A., Burmeister F., Albus R.: *Contribution of LNG use for the low calorific natural gas network's safe and sustainable operation*. Energy Procedia **64**(2015), 83–90. doi: [10.1016/j.egypro.2015.01.011](https://doi.org/10.1016/j.egypro.2015.01.011)
- [42] <https://www.cumminswestport.com/models/isx12-g> (accessed Oct. 16, 2018).
- [43] Davis S.G., Law C.K.: *Determination of fuel structure effects on laminar flame speeds of C₁ to C₈ hydrocarbons*. Combust. Sci. Technol. **140**(1998), 1–6, 427–449. doi: [10.1080/00102209808915781](https://doi.org/10.1080/00102209808915781)
- [44] Sutton J.A., Williams B.A., Fleming J.W.: *Investigation of NCN and prompt-NO formation in low-pressure C₁-C₄ alkane flames*. Combust. Flame **159**(2012), 2, 562–76. doi: [10.1016/j.combustflame.2011.08.023](https://doi.org/10.1016/j.combustflame.2011.08.023)
- [45] Lamoureux N., Desgroux P., Bakali A., Pauwels J.F.: *Experimental and numerical study of the role of NCN in prompt-NO formation in low-pressure CH₄-O₂-N₂ and C₂H₂-O₂-N₂ flames*. Combust. Flame **157**(2010), 1929–1941. doi: [10.1016/j.combustflame.2010.03.013](https://doi.org/10.1016/j.combustflame.2010.03.013)